Proceedings of the 2006 IEEE
International Conference on Control Applications
Munich, Germany, October 4-6, 2006

Optimal Power Split in Fuel Cell Hybrid Electric Vehicle with different Battery Sizes, Drive Cycles, and Objectives

Olle Sundström and Anna Stefanopoulou

Abstract— **This paper explores different hybridization levels of a vehicle powered by a polymer electrolyte membrane fuel cell stack. The energy buffer considered is a lead-acid type battery. The effects of the battery size on hydrogen consumption and stack dynamic loading for different drive cycles are determined when dynamic programming determines the optimal current drawn from the fuel cell stack system. The optimal power split policies are analyzed to quantify all the energy losses and their paths in an effort to clarify the hybridization needs for a fuel cell vehicle.**

I. INTRODUCTION

There are two main advantages to hybridize a vehicle equipped with a fuel cell system (FCS): 1) Decouple the fuel cell stack from the voltage and current demands from the traction motor to allow the FCS to operate as close to optimally as possible. 2) Recover energy when decelerating and braking through regenerative braking.

Although these reasons are identical to the reasons for hybridizing an internal combustion engine (ICE) vehicle, the fuel cell stack operation differs from the operation of an ICE. Fuel cells operate at high efficiencies for a wide range of operating conditions. If not considering the regenerative braking, it is not trivial if and how much a FCS vehicle can benefit from allowing the FCS to operate as close to an optimum as possible. The benefits can be categorized as increased fuel economy or reduced reactant starvation periods due to battery assisting the FCS. The latter reason for FCS hybridization differs from those to hybridize an Internal Combustion Engine vehicle [1] [2].

When hybridizing a power train it is challenging to size the energy buffer (EB) because the drive cycle [2] [3], the control policy [4], and the hardware architecture [5] affect the optimal size. The type and characteristics of the energy buffer used to control the power split also affect the EB sizing. When increasing the EB size in a Hybrid Electric Vehicles the total vehicle weight increases which affects the fuel consumption. EB sizing is therefore an important issue to consider when developing hybrid electric vehicles.

In this study the effects of different lead-acid battery sizes have been analyzed for two separate cases. First, when deviations from the optimum state of charge and hydrogen consumption are considered. Second, when the FCS oxygen excess ratio is included in the optimization. This is done to separate the benefits from allowing the Fuel Cell to operate as optimally as possible from the benefits of assisting the Fuel Cell during load transients.

When making the decision to include a battery or other energy buffer in the power train, it is important to consider the actual costs of the battery and the added complexity associated with hybridization [2] [6]. The prices on fuel cells and batteries varies with time, we will therefore only focus on determine the effects of hybridization on fuel consumption and stack oxygen excess ratio (OER). We do not know how detrimental to the FCS life are periods of low excess oxygen ratio thus we choose an arbitrary function to penalize deviations of OER.

Section II describes the Fuel Cell Hybrid Electric Vehicle (FCHEV) model together with the strategy used to control the power split. Section III shows the results. Finally, in Section IV, the conclusions from the results and future work are discussed.

II. METHOD

To investigate how different battery sizes affect the FCHEV performance an optimal control approach is used. By using this approach different sizes are evaluated and compared regarding their optimal performances on known drive cycles. Dynamic Programming (DP) [7] is used to optimally control the power split between the FCS and the battery. This section describes the FCHEV model, the DP method, and the drive cycles that were used to evaluate the component sizes.

A. Model

The FCHEV model is separated into three components; Fuel Cell System, Battery, and Vehicle. This section explains how each component is modeled and how they interact with each other. An overview of the model, its components, and the signal flow during the DP optimizations is shown in Fig. 1 In this study the energy losses in the power train, DC motor, inverter, and the DC/DC converter have been neglected. The FCHEV model is a simplified version of the detailed model in [1].

DP complexity is exponential in the number of states in the model, it is therefore crucial to minimize the number of states and the computation time of the model. This is done by approximating fast dynamics as instantaneous and employing nonlinear static maps to model their associated steady state behavior. For example, in the original model [1] the DC/DC converter comprises of second order system dynamics coupled with a proportional controller that controls

This work is supported by the National Science Foundation (NSF) CMS-0201332 and the Automotive Research Center (ARC)

O. Sundström is fulfilling his M.Sc. Thesis requirement at the Department of Signals and Systems, Chalmers University of Technology, Sweden

A. Stefanopoulou is with the Department of Mechanical Engineering, University of Michigan, USA

0-7803-9796-7/06/$20.00 ©2006 IEEE

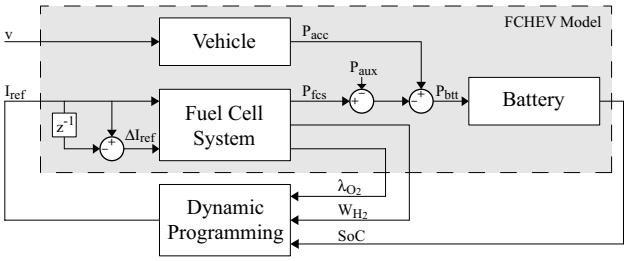

Fig. 1. Fuel Cell hybrid electric vehicle components and the signal flow during the dynamic programming optimizations.

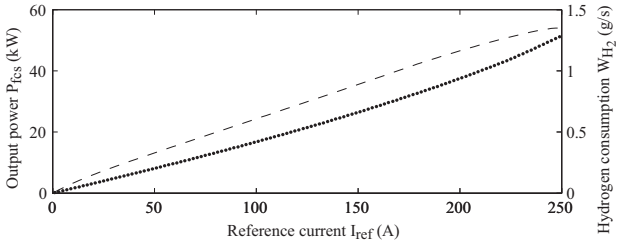

Fig. 2. Fuel Cell System output power, P_{fcs}, (dashed) and hydrogen consumption, W_{H_2}, (dotted) map.

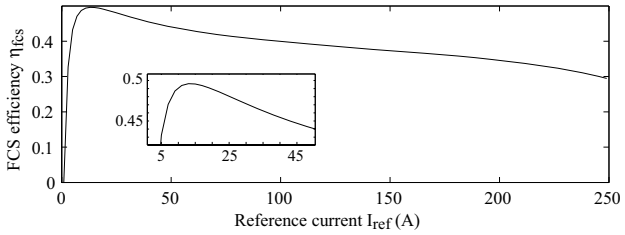

Fig. 3. Fuel Cell System efficiency, η_{fcs}, using the higher heating value energy content of hydrogen.

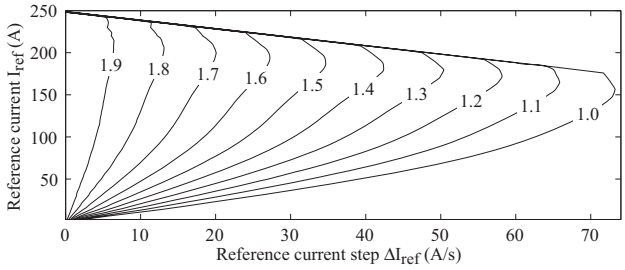

Fig. 4. Oxygen Excess Ratio map used to calculate the OER in the Fuel Cell System when changing the reference current.

the output current from the FCS. In this study the dynamics of the DC/DC converter are assumed to be fast and hence the net current out from the FCS is the same as the DC/DC converter controller current setpoint (input to the DC/DC converter controller). The parameters for each component in the model are shown in Table I.

1) Vehicle: The vehicle is a midsized car with a mass of 1384 kg with the FCS and hydrogen storage and without the mass of the battery pack. The forces affecting vehicle motion are the output force from the drive train, rolling resistance, and air drag. The power demand, P_{dem}, is calculated using the known drive cycle speeds together with

$$P_{dem}(m,t) = v(t)(m\dot{v}(t) + F_f(m) + F_d(v(t))), \qquad (1)$$

where the rolling resistance is

$$F_f(m) = K_f mg,$$

and the air drag is

$$F_d(v(t)) = \frac{\rho_{air} C_d A}{2} v^2(t).$$

The acceleration power demand, P_{acc} in (2), which is the positive part of the power demand, P_{dem}, is provided by the Fuel Cell System and the battery pack

$$P_{acc}(m) = \begin{cases} P_{dem}(m) & P_{dem}(m) \geq 0 \\ 0 & P_{dem}(m) < 0. \end{cases} \qquad (2)$$

Regenerative braking has not been addressed in this paper. The road is assumed to be flat, and hence there is no force from the road grade.

2) Fuel Cell System: The FCS is the energy source in the vehicle. It converts the energy in the fuel (hydrogen) to electric energy in the vehicle. The current drawn from the FC stack, I_{st}, is calculated using

$$I_{st} = I_{ref} + \frac{P_{cm}}{V_{st}},$$

where I_{ref} is the net current out of the FCS and V_{st} is the stack voltage which is a function of temperature, partial pressure of hydrogen and oxygen, and the stack current I_{st} [8]. The current necessary to drive the FC compressor, P_{cm}/V_{st}, is the largest parasitic loss in the FCS and is calculated based on the compressor absorbed power P_{cm} and the voltage at the compressor terminals. The compressor absorbed power, P_{cm}, is calculated using nonlinear compressor maps [8]. The FCS output power is calculated using

$$P_{fcs} = V_{st} \cdot I_{ref}.$$

The FCS power output map, generated from the FCS model [1], used in this paper is shown in Fig. 2. The hydrogen consumption, shown also in Fig. 2, is calculated using

$$W_{H_2} = \frac{I_{st} \cdot n_{cell} \cdot M_{H_2}}{2\ F},$$

where n_{cell} is the number of cells in the stack, M_{H_2} is the molar mass of hydrogen, and F is Faraday's constant. The FCS efficiency is defined as

$$\eta_{fcs} = \frac{P_{fcs} - P_{aux}}{Q_{HHV} \cdot W_{H_2}}, \qquad (3)$$

where Q_{HHV} is the higher heating value of hydrogen and P_{aux} is a fixed power demand from all the other FCS auxiliary devices. The efficiency of the FCS, η_{fcs}, for different

reference currents is shown in Fig. 3. The average FCS efficiency for an entire drive cycle is defined as

$$\bar{\eta}_{fcs} = \frac{E_{fcs}}{E_{H_2}}, \tag{4}$$

where E_{fcs} is the total energy out from the FCS and E_{H_2} is the total energy in the used fuel

$$E_{fcs} = \int_0^T (P_{fcs} - P_{aux})\, dt$$

$$E_{H_2} = Q_{HHV} \cdot \int_0^T W_{H_2}\, dt. \tag{5}$$

An important performance variable for Fuel Cells is the OER in the cathode which is regulated by the compressor to a nominal value of 2 with a feedforward map [1]. However due to the dynamics of the manifold filling and the compressor dynamics the OER drops when changing the reference current before regulation at a steady-state of 2 is archived. To capture OER deviations from the nominal steady-state value, which only occurs during current transients, we introduce an extra state and develop the map in Fig. 4. This map is calculated using the original FCS model which includes the dynamics of compressor and manifolds. The OER values in the map are the minimum OER for different changes in the reference current, ΔI_{ref}. For example, a step increase from 100 A to 110 A causes OER to drop momentarily down to 1.8, whereas a step from 100 A to 120 A causes an OER drop to 1.6.

3) Battery Pack: The battery pack is modeled as a voltage source in series with a resistance and is based on an ADVISOR model [9]. The battery output/input power, P_{btt}, which is the remaining power to meet the drive cycle acceleration power demand, P_{acc}, is calculated using

$$P_{btt} = P_{acc} - (P_{fcs} - P_{aux}).$$

The battery current, I_{btt}, is calculated using

$$I_{btt} = \frac{V_{oc} - \sqrt{V_{oc}^2 - 4 \cdot R_{int} \cdot P_{btt}}}{2 \cdot R_{int}},$$

where V_{oc} is the open circuit voltage of the battery and R_{int} is the battery's internal resistance. The open circuit voltage and the internal resistance are functions of the state of charge and the number of modules used in the battery pack. The open circuit voltage and the internal resistance for a single module are shown in Fig. 5. The battery's state of charge (SoC) is calculated using

$$\frac{d}{dt}(SoC) = \begin{cases} \frac{-I_{btt}}{3600 \cdot q_{btt}} & I_{btt} \geq 0 \\ \eta_{btt} \cdot \frac{-I_{btt}}{3600 \cdot q_{btt}} & I_{btt} < 0, \end{cases}$$

where η_{btt} is the battery charging efficiency and q_{btt} is the battery capacity (Table I). The initial condition of the state of charge is set to $SoC(0) = SoC_{ref} = 0.6$.

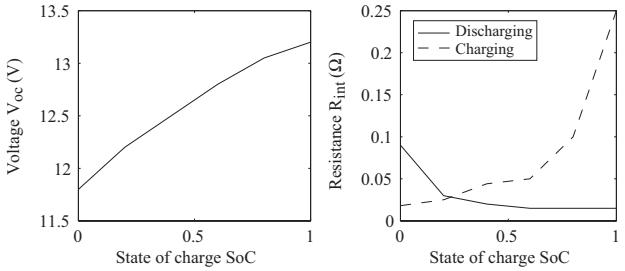

Fig. 5. Battery module characteristics: The open circuit voltage (left) and internal resistance (right) both when charging (dashed) and when discharging (solid)

TABLE I
MODEL PARAMETERS

FUEL CELL SYSTEM

Cells (n_{cell})	381
Maximum net power	54 kW
Auxiliary power (fixed) (P_{aux})	500 W
OER limit ($\lambda_{O_2}^{lim}$)	1.75

BATTERY MODULE

Mass (m_{btt})	6.68 kg
Capacity (q_{btt})	18 Ah
Maximum power ($SoC = 0.6$)	2.78 kW
Charging efficiency (η_{btt})	0.9
SoC reference (SoC_{ref})	0.6

VEHICLE

Mass (without battery) (m_0)	1384 kg
Rolling resistance coefficient (K_f)	0.02
Aerodynamic drag coefficient (C_d)	0.312
Frontal area (A)	2.06 m^2

B. Dynamic Programming

DP can be used to numerically solve optimal control problems. DP can be used in both stochastic and deterministic systems. When using Stochastic Dynamic Programming (SDP), to optimally control the power split in a hybrid electric vehicle, the power demand is often described as a Markov chain. This stochastic model can be estimated from several standard drive cycles [4] or from real world measurements [10]. SDP has the advantage over Deterministic Dynamic Programming (DDP) that the resulting control law is causal. In this study, however, we will use DDP and optimize the battery size separately for different drive cycles to show the drive cycle's effect on the battery sizing. The FCHEV model can be described as the nonlinear state space model

$$\dot{\mathbf{x}} = f(\mathbf{x}, u, w),$$

with the states

$$x_1 = SoC,\ x_2 = I_{ref} = u,$$

the input reference current u, and the power demand w. The third state, v, in the model is not included when using the DP because the power demand is precalculated using the vehicle model. Forward Euler approximation is used to discretize

the continuous in time state equations before using DP. The variables $\mathbf{x}$, u, and w are limited to the finite spaces $\mathbf{X}$, U, and W

$$\mathbf{x} \in \mathbf{X},\ u \in U,\ w \in W.$$

To optimally control this system using the DDP algorithm, (6) needs to be minimized, where $J(\mathbf{x}(\tau), u(\tau), w(\tau))$ is the cost function to use the input u at the state $\mathbf{x}$ with the power demand w at time τ

$$\sum_{\tau=0}^{\tau=K} J(\mathbf{x}(\tau), u(\tau), w(\tau)) \rightarrow min. \tag{6}$$

The cost J is calculated using

$$J = (\alpha \cdot \Delta SoC)^2 + \beta \cdot W_{H_2} + (\gamma \cdot \Delta\lambda_{O_2})^2 \tag{7}$$

$$\Delta SoC = SoC - SoC_{ref}$$

$$\Delta\lambda_{O_2} = \begin{cases} \lambda_{O_2}^{lim} - \lambda_{O_2}, & \lambda_{O_2} < \lambda_{O_2}^{lim} \\ 0, & \lambda_{O_2} \geq \lambda_{O_2}^{lim}, \end{cases}$$

where ΔSoC is the deviation of the battery's state of charge from the reference value SoC_{ref}, W_{H_2} is the hydrogen consumption in the FCS, $\Delta\lambda_{O_2}$ is the deviation of OER below a limiting value $\lambda_{O_2}^{lim}$, and (α, β, and γ) are weights.

To minimize (6) we need to define the optimal cost-to-go function which is the minimum cost to go from the state $\mathbf{x}$ at the time k to time K

$$V(\mathbf{x}, k) = \min_{u(k), u(k+1), \ldots, u(K)} \sum_{\tau=k}^{\tau=K} J(\mathbf{x}(\tau), u(\tau), w(\tau)) \tag{8}$$

with the final penalty $V(\mathbf{x}, K) = \delta \Delta SoC^2$. The final state $\mathbf{x}$ at time K is penalized to ensure that the final state of charge is close to the initial state of charge.

If Q is the cost of using input u from state $\mathbf{x}$ at time k together with the optimal cost-to-go from the resulting state from time $k+1$

$$Q(\mathbf{x}, u, k) = J(\mathbf{x}, u, w(k)) + V(\mathbf{x}(k+1), k+1),$$

then the minimum cost-to-go function can be written like

$$V(\mathbf{x}, k) = \min_u Q(\mathbf{x}, u, k).$$

The optimal control input is the argument which minimizes Q

$$u(k) \in \operatorname{argmin}_u Q(\mathbf{x}, u, k).$$

By discretizing the finite spaces $\mathbf{X}$, U, and W and by recursively calculating V for all k, $\mathbf{x}$, and u the optimal control sequence is given by the arguments which minimized Q.

C. Drive Cycles

The power demand from the drive cycles is calculated backwards using the discretized version of the vehicle model (1). The three drive cycle are: New York City Cycle which represents low speed and mild driving, FTP-72 cycle which represents both low speed city driving and moderate highway driving, and SFTP which represents aggressive high speed driving. The drive cycles, and their power characteristics for a vehicle with 10 battery modules and a mass of 1451 kg, are summarized in Table II.

TABLE II
DRIVE CYCLE CHARACTERISTICS

	Power (kW)					
	Average		Max			
Cycle	Acc.	Brk.	Acc.	Brk.	Top speed	Duration
NYCC	4.9	4.1	25.7	21.6	44.6 km/h	599 s
FTP-72	7.2	7.0	31.8	23.4	91.3 km/h	1370 s
SFTP	21.5	17.3	80.1	53.8	129.2 km/h	601 s

III. RESULTS

This section shows the results from the DP optimizations. We will focus on the energy losses in the different components and how they change with the battery size. These results are separated into two parts. First without penalizing on the OER and second when including the OER in the cost function.

A. Without OER penalty

This section shows the results when disregarding the OER. This is done by only including the fuel consumption and the state of charge deviation in the cost function (7) ($\gamma = 0$). The weights α and β in (7) are set so that when $\Delta SoC = 0.1$ and $W_{H_2} = 0.0013$kg/s then $(\alpha \Delta SoC)^2 = \beta W_{H_2} = J/2 = 1$, i.e. each performance variable contributes equally to the cost. We will show how and why the FCS efficiency changes when increasing the battery size. Moreover we will show the energy lost by charging/discharging the battery and the energy lost due to added weight with increasing battery size.

1) Fuel Cell System: An example of how DP uses the FCS for a vehicle with 10 battery modules for the medium drive cycle is shown in Fig. 6. Under these conditions 50% of the reference current values are between 7 A and 22 A, 95% between 4.7 A and 66 A, and 100% between 2 A and 111 A. The resulting average FCS efficiency (4) for this configuration is 46.1%. The average FCS efficiency for different battery sizes is shown in the left column of Fig. 7. When increasing the battery size the average FCS efficiency increases. This increase is accomplished through the decoupling between the acceleration power demand, P_{acc}, and the FCS output power, P_{fcs}. In particular, the right column of Fig. 7 shows that the FCS operates more often at reference current levels with higher efficiency. The right column of Fig. 7 shows the distribution regions of the FCS reference current for different sizes together with the FCS efficiency curve (3). Note that the figures in the right column

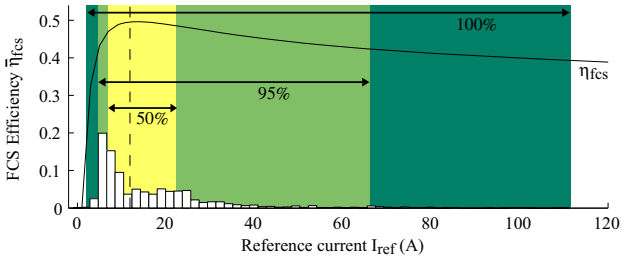

Fig. 6. The FCS reference current, I_{ref}, distribution and the FCS efficiency, η_{fcs}, for a vehicle with 10 modules for the medium (FTP-72) drive cycle. The reference current median value (dashed) together with the regions (50%, 95%, and 100%) around this median.

of Fig. 7 condense the information in Fig. 6 (switched axes) for different battery sizes.

For the mild cycle, the FCS operates at low current levels and adding battery modules improves the FCS efficiency. In fact, the FCS efficiency improvement observed in the mild cycle is the largest of all cycles. This significant improvement can be explained as follows. More than 50% of the reference current levels is at the low levels below the optimal FCS current level. Operating the FCS with very low currents is very inefficient so there is a large increase in FCS efficiency when DP stores energy in the battery and shifts the low current levels drawn from the FCS towards higher current regions. For the medium cycle there is less need for operation in the low efficient region of very small currents. The vehicle will therefore not benefit as much as for the mild cycle when increasing the battery size. The small FCS efficiency improvements are, in fact, realized by reducing the peak reference currents. Note that at least 10 battery modules are needed to satisfy the acceleration demand in the aggressive cycle.

2) Battery: The electrical energy loss in the battery is defined as

$$E_{loss}^{btt} = \left| \int_0^T P_{btt}\, dt \right|, \tag{9}$$

where P_{btt} is the battery power. To be able to compare the total energy loss in the vehicle and the battery energy loss we need to define the hydrogen equivalent energy loss $E_{loss}^{btt}/\bar{\eta}_{fcs}$. This is the hydrogen energy required to produce the electric energy lost in the battery. The energy loss in the battery, E_{loss}^{btt}, together with the hydrogen equivalent energy loss, $E_{loss}^{btt}/\bar{\eta}_{fcs}$, is shown in the left column of Fig. 8.

It is not easy to analyze the energy loss in the battery as the battery size increase for the different cycles because the power split is decided through the DP policy and not through a rule-based controller. Specifically, the DP uses the battery to save some energy by allowing the FCS to operate more efficiently and will waste some this energy in the battery.

3) Added Mass: The energy loss due to the added mass, when increasing the battery size, affects the performance of the vehicle. It is therefore important to separate the losses due to the added weight from the other losses. We define the

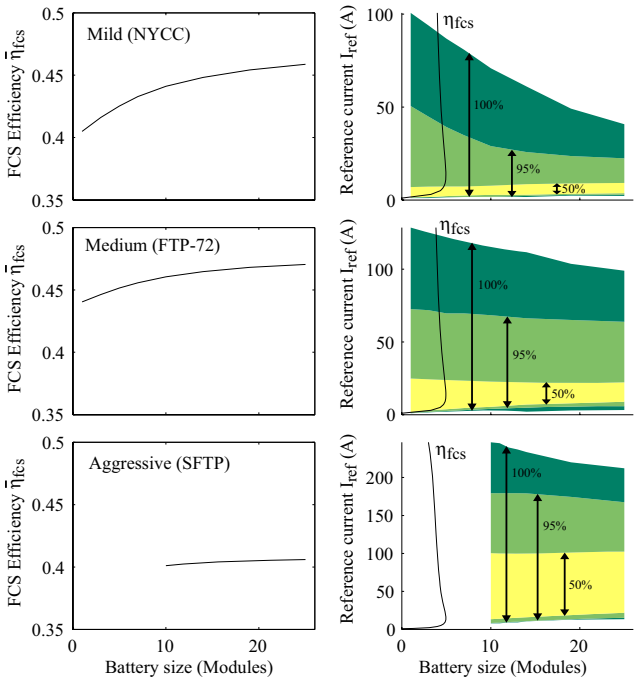

Fig. 7. Average FCS efficiency, $\bar{\eta}_{fcs}$, (left) together with the reference current distribution (right) for different battery sizes and drive cycles (without OER constraints). The FCS efficiency curve is shown in the left part of the reference current distribution plot.

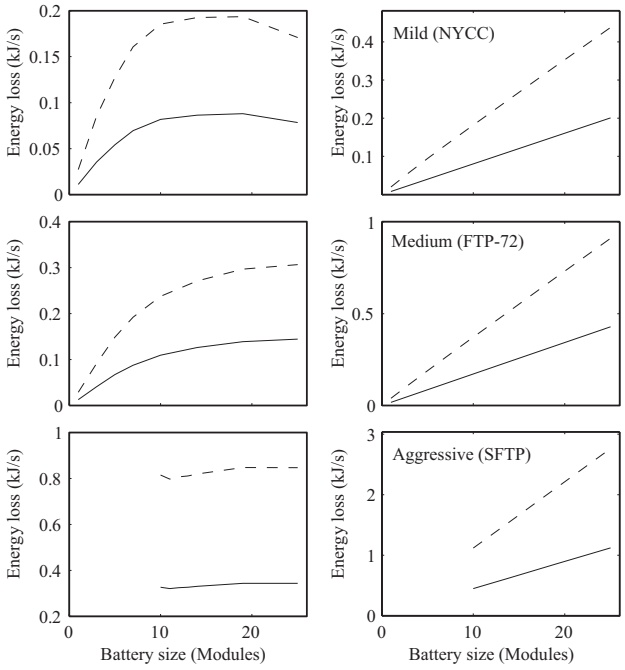

Fig. 8. Average battery energy loss, E_{loss}^{btt}, (solid,left) and its equivalent hydrogen energy loss, $E_{loss}^{btt}/\bar{\eta}_{fcs}$, (dashed,left) together with the average energy loss due to the added mass, E_{loss}^{m}, (solid,right) and its equivalent hydrogen energy loss, $E_{loss}^{m}/\bar{\eta}_{fcs}$, (dashed,right) (without OER penalty).

energy loss due to the added weight as

$$E^m_{loss} = E^m_{acc} - E^{m_0}_{acc} \tag{10}$$

$$E^m_{acc} = \int_0^T P_{acc}(m_0 + n_{btt} \cdot m_{btt})\, dt$$

$$E^{m_0}_{acc} = \int_0^T P_{acc}(m_0)\, dt, \tag{11}$$

where $P_{acc}(m_0)$ is the acceleration power demand (2) for a vehicle without any battery and $P_{acc}(m_0 + n_{btt} \cdot m_{btt})$ is the acceleration power demand for a vehicle with n_{btt} battery modules. The parameters m_0 and m_{btt} are shown in Table I. The energy loss due to the added mass E^m_{loss} and the hydrogen equivalent energy loss $E^m_{loss}/\bar{\eta}_{fcs}$ are shown in the right column of Fig. 8. The energy loss E^m_{loss} is increasing proportional to the battery size for all three drive cycles. The hydrogen equivalent energy loss is increasing slightly faster for smaller battery sizes for the mild and the medium drive cycles due to the changing FCS efficiencies in Fig. 7. Note here that an increase in battery size corresponds to an increase in vehicle weight and net vehicle power because the FCS power size remains fixed. In future work this study could be performed under fixed vehicle net power by resizing battery and FCS simultaneously. Resizing the FCS depend on scalable FCS auxiliary losses and associated transient response.

4) System: To compare the losses in the battery and the losses due to the added weight to the remaining losses in the FCS we define the total hydrogen energy loss for a cycle

$$E^0_{loss} = E_{H_2} - E^{m_0}_{acc},$$

where E_{H_2} is the total energy in the used fuel defined in (5) and $E^{m_0}_{acc}$ is the energy defined in (11). So E^0_{loss} corresponds to the hydrogen chemical energy used minus the energy required to power the original vehicle mass through the drive cycle. The total hydrogen energy loss can be separated into three parts

$$E^0_{loss} = \frac{E^{fcs}_{loss}}{\bar{\eta}_{fcs}} + \frac{E^{btt}_{loss}}{\bar{\eta}_{fcs}} + \frac{E^m_{loss}}{\bar{\eta}_{fcs}},$$

where $E^{btt}_{loss}/\bar{\eta}_{fcs}$ is the hydrogen equivalent energy loss in the battery, $E^m_{loss}/\bar{\eta}_{fcs}$ is the hydrogen equivalent energy loss due to the added mass, and $E^{fcs}_{loss}/\bar{\eta}_{fcs}$ is the remaining hydrogen equivalent energy loss in the FCS. The electric energy loss in the battery, E^{btt}_{loss}, is defined in (9) and the electric energy loss due to added weight is defined in (10). The remaining electric energy loss in the FCS is then calculated using

$$E^{fcs}_{loss} = \bar{\eta}_{fcs} E^0_{loss} - E^{btt}_{loss} - E^m_{loss},$$

where $\bar{\eta}_{fcs} E^0_{loss}$ can be seen as the total electric energy lost.

These energy losses are shown in Fig. 9. For the mild cycle the large increase in FCS efficiency at first reduces the total energy loss when increasing the battery size. For larger battery sizes, though, the loss due to the added weight increases more than the other losses decreases. Therefore, the

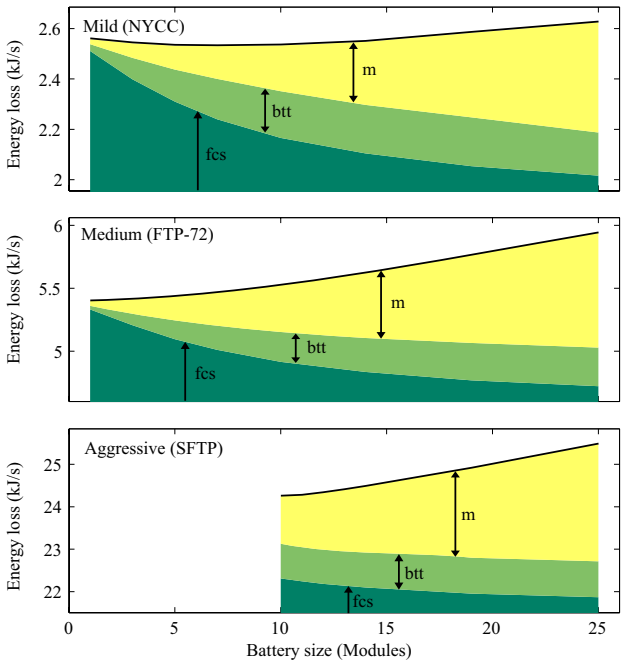

Fig. 9. The average energy loss per second in the three drive cycles (without OER penalty). Equivalent hydrogen energy loss from added weight $E^m_{loss}/\bar{\eta}_{fcs}$ (m), equivalent hydrogen energy loss in the battery $E^{btt}_{loss}/\bar{\eta}_{fcs}$ (btt), and the FCS hydrogen equivalent energy loss $E^{fcs}_{loss}/\bar{\eta}_{fcs}$ (fcs)

mild cycle has an optimal battery size of around 7 modules. For the medium cycle the FCS efficiency does not increase enough to compensate for the added weight and it is therefore no point in adding a battery to the vehicle. In the aggressive cycle there is a minimum battery size of 10 modules to meet the high power demand (Table. II). However, there is no reduction in the total energy lost due to the increasing energy lost due to the added battery weight. Thus, to the contrary of hybridizing an ICE vehicle, hybridization of a Fuel Cell vehicle cannot always be justified based solely on fuel consumption improvements.

B. With OER penalty

This section shows the DP results OER deviations are penalized. This is done by including the fuel consumption, the state of charge deviation, and the OER in the cost function (7). The weights α, β, and γ in (7) is set so that when $\Delta SoC = 0.1$, $W_{H_2} = 0.0013$kg/s, and $\Delta\lambda_{O_2} = 0.25$ then $(\alpha\Delta SoC)^2 = \beta W_{H_2} = (\gamma\Delta\lambda_{O_2})^2 = J/3 = 1$, i.e. each performance variable contributes equally to the cost. An OER limit, $\lambda^{lim}_{O_2} = 1.75$ has been used throughout this section. We will show how DP adjusts the FCS reference current and the implications of the DP decisions on the FCS efficiency, the energy loss in the battery, and the energy loss due to the added weight with increasing battery size for the different drive cycles.

1) Fuel Cell System: The FCS efficiency (4) is shown in the left column of Fig. 10. When increasing the battery size the FCS efficiency increases. This increase is caused, as in the case without OER penalty, by decoupling the acceleration

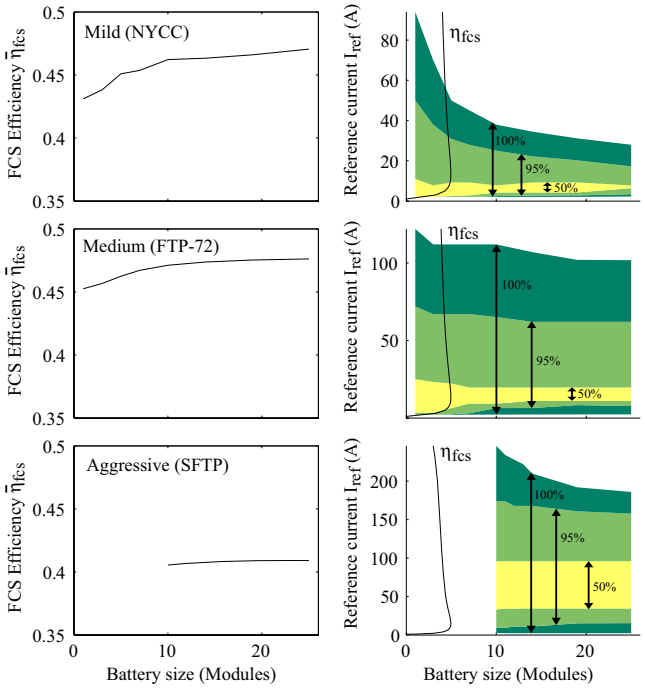

Fig. 10. Fuel Cell System efficiency, $\bar{\eta}_{fcs}$, (left) together with the reference current distribution (right) for different battery sizes and drive cycles (with OER penalty). The FCS efficiency curve is shown in the left part of the reference current distribution plot.

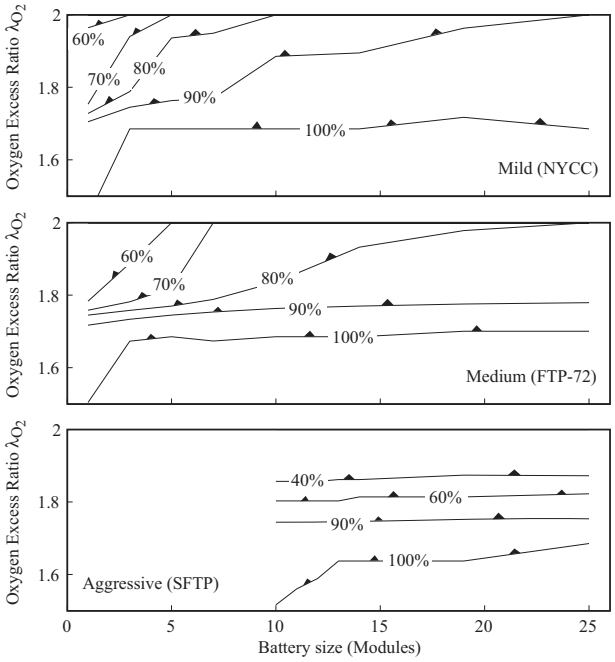

Fig. 11. The OER distributions for different battery sizes for the three drive cycles. The percentages gives how much of the time is spent above the OER values.

power demand, P_{acc}, from the Fuel Cell output power, P_{fcs}. The right column of Fig. 10 shows the distribution of the FCS reference current, I_{ref}, for different sizes together with the FCS efficiency curve, η_{fcs} (3). The changes of these distributions are similar to those when not including the OER penalty in the cost function. When increasing the battery size the DP shifts the inefficient current levels towards higher efficiencies. The average FCS efficiencies achieved now are larger than the ones observed when OER was not penalized because the peak reference current and very low reference current levels that typically cause large OER excursions are now rare. The peak reference current now shift to lower values with high FCS efficiency as shown in Fig. 10 (right column). The resulting OER distributions for the different drive cycles and battery sizes are shown in Fig. 11. For example, with a battery size of 5 modules in the medium cycle (FTP-72) the OER is higher than 1.8 70% of the time and higher than 1.68 100% of the time. Furthermore, with a battery size of 19 modules in the mild cycle (NYCC) the OER is higher than 1.7 100% of the time and higher than 1.95 90% of the time.

2) Battery: The energy loss in the battery, E^{btt}_{loss}, together with the hydrogen equivalent energy loss, $E^{btt}_{loss}/\bar{\eta}_{fcs}$, when including the OER are shown in the left column of Fig. 12.

For the mild and medium cycles the battery energy loss decreases rapidly at first but then levels out for larger battery sizes. For the aggressive cycle the battery energy loss is also decreasing with increasing battery size. This is because the DP is forced, through the added cost in (7), to use the battery to maintain the OER at a high levels. This is hard for small batteries and will therefore result in larger losses in the battery.

3) Added Mass: The energy losses due to the added mass, when increasing the battery size, are the same when including the OER as when not including the OER. The hydrogen equivalent energy loss is slightly different when including the OER due to the higher average FCS efficiencies. These energy losses are shown in Fig. 12.

4) System: The total hydrogen energy loss, the hydrogen equivalent energy loss due to the added weight, and the hydrogen equivalent energy loss in the battery are shown in Fig. 13. For the mild cycle the large energy loss in the battery for small battery sizes makes it inefficient to have less battery modules than 7. For the medium cycle the large energy loss in the battery for small battery sizes together with the large energy loss due to the added weight for large batteries introduce an optimal battery size of 5 to 10 modules. In the aggressive cycle the decrease in battery energy loss is almost equivalent to the energy loss due to added weight. However there is an optimal battery size of 12 modules.

IV. CONCLUSIONS AND FUTURE WORK

For the considered vehicle, fuel cell system and battery this paper shows that without OER penalty there is no need for hybridization for the medium and aggressive drive cycles. Even if the power split is optimally controlled the increased FCS efficiency does not make up for the losses from added weight. There is however an optimal battery size for the mild drive cycle due to eliminating the need for operating the FCS at extremely low reference currents where the FCS auxiliary

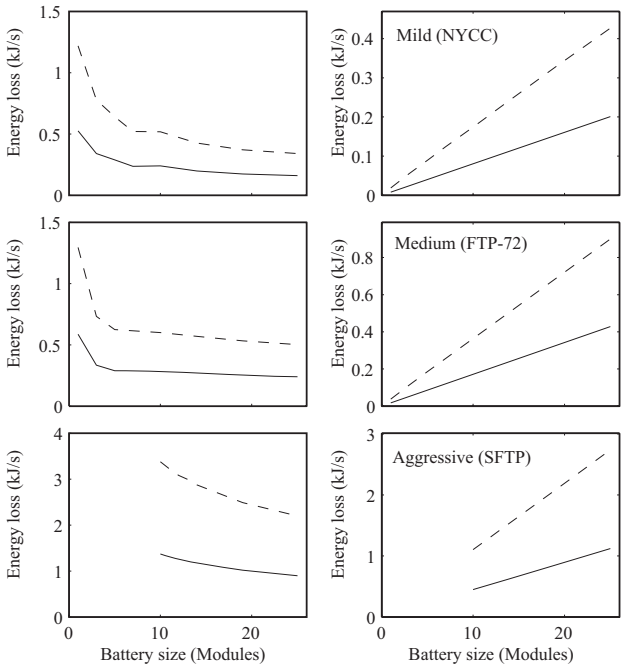

Fig. 12. Average battery energy loss, E^{btt}_{loss}, (solid,left) and its equivalent hydrogen energy loss, $E^{btt}_{loss}/\bar{\eta}_{fcs}$, (dashed,left) together with the average energy loss due to the added mass, E^{m}_{loss}, (solid,right) and its equivalent hydrogen energy loss, $E^{m}_{loss}/\bar{\eta}_{fcs}$, (dashed,right) (with OER penalty).

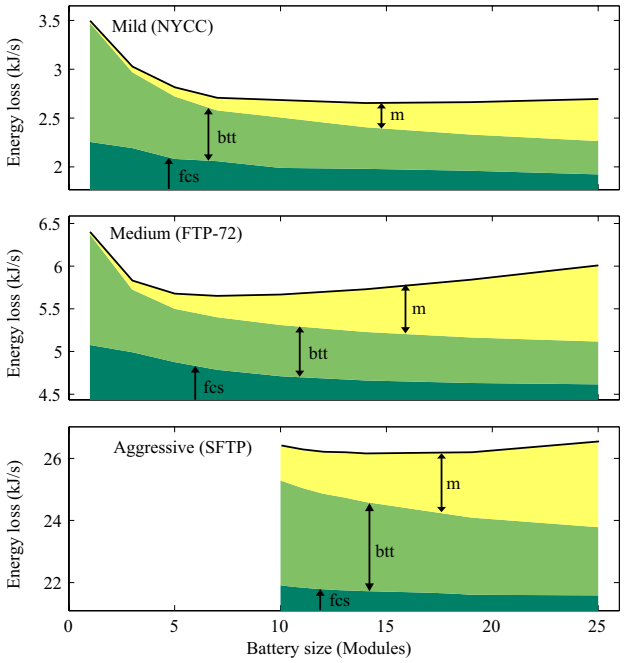

Fig. 13. The average energy loss per second in the three drive cycles (with OER penalty). Equivalent hydrogen energy loss from added weight $E^{m}_{loss}/\bar{\eta}_{fcs}$ (m), equivalent hydrogen energy loss in the battery $E^{btt}_{loss}/\bar{\eta}_{fcs}$ (btt), and the FCS hydrogen equivalent energy loss $E^{fcs}_{loss}/\bar{\eta}_{fcs}$ (fcs)

losses are dominating. When OER is taken into account then hybridization is beneficial far all three cycles.

We can see that hybridization offers a greater benefit for the mild (NYCC) drive cycle than for the medium (FTP-72) and aggressive (SFTP) drive cycles regardless if including the OER constraints or not. This results match the results shown in [2].

The optimal battery size is dependent on the cycle, the vehicle weight, the type of battery and energy density of the battery. Thus, this study is very specific to our configuration, the specific weights and characteristics of the vehicle and its different components. Furthermore, the model used in this study is very simple and does not consider mechanical losses in the power train.

The results can however be seen as an indication of how the optimal battery size change when limiting the FCS transient loading. The added weight is the factor which makes configurations with larger batteries perform worse, it is therefore crucial to increase the power-to-weight ratio of the batteries.

The future work includes battery sizing when including regenerative braking and when varying the efficiency of the regenerative braking. A comparison between battery sizing with a rule-based power split controller will show how much the predictiveness of the DP method affects the optimal size.

REFERENCES

[1] K-W. Suh and A. G. Stefanopoulou. Effects of control strategy and calibration on hybridization level and fuel economy in fuel cell hybrid electric vehicle. *SAE Paper 06P-428*, 2006. To be published.

[2] D. J. Friedman. Maximizing direct-hydrogen pem fuel cell vehicle efficiency - is hybridization necessary. *SAE Paper*, SP-1425, 1999.

[3] T. Matsumoto, N. Watanabe, H. Sugiura, and T. Ishikawa. Development of fuel-cell hybrid vehicle. *SAE Paper 2002-01-0096*, SP-1691, 2002.

[4] C. C. Lin, H. Peng, and J. W. Grizzle. A stochastic control strategy for hybrid electric vehicles. *Proceedings of the American Control Conference*, 2004. Boston, MA.

[5] T. Ishikawa, S. Hamaguchi, T. Shimizu, T. Yano, S. Sasaki, K. Kato, M. Ando, and H. Yoshida. Development of next generation fuel-cell hybrid system - consideration of high voltage system. *SAE Paper 2004-01-1304*, SP-1827, 2004.

[6] K. S. Jeong and B. S. Oh. Fuel economy and life-cycle cost analysis of a fuel cell hybrid vehicle. *Journal of Power Sources*, 105:58–65, 2002.

[7] R. E. Bellman. *Dynamic Programming*. Princeton University Press, 1957.

[8] J. T. Pukrushpan, H. Peng, and A. G. Stefanopoulou. Control-oriented modeling and analysis for automotive fuel cell systems. *ASME Journal os Dynamic Systems, Measurement, and Control*, 126(1):14–25, 2004.

[9] V. H. Johnson. Battery performance models in advisor. *Journal of Power Sources*, 110:321–329, 2002.

[10] L. Johannesson, M. Åsbogård, and B. Egardt. Assesing the potential of predictive control for hybrid vehicle powertrains using stochastic dynamic programming. *IEEE Proceedings of the Intelligent Transportation Systems*, 2005.